AIMS Energy, 13(4): 798–818.
DOI: 10.3934/energy.2025029
Received: 26 January 2025
Revised: 24 May 2025
Accepted: 24 June 2025
Published: 08 July 2025

https://www.aimspress.com/journal/energy

Research article

A virtual power plant scheduling strategy considering cooperative participation of multiple industrial users in demand response

Long Wang[1], Tingzhe Pan[2,*], Yi Wang[1], Xin Jin[2], Heyang Yu[2] and Wangzhang Cao[2]

[1] Department of Sales & Marketing, China Southern Power Grid Co., Ltd., Guangzhou 510663, China
[2] Electric Power Research Institute , China Southern Power Grid Co., Ltd., Guangzhou 510663, China

* **Correspondence:** Email: 18900220639@163.com; Tel: +86-18900220639.

Abstract: The construction of a novel power system requires the full utilization of demand-side flexibility. Industrial users, as the primary electricity consumers in society, play a critical role in system regulation. However, industrial users often participate in demand response (DR) as individual entities, and their single-unit regulation capacity is limited, making it difficult to effectively mobilize the regulation potential of a large number of industrial users. These issues hinder the effective use of demand-side flexibility. To address these problems, this paper proposes a method where a virtual power plant (VPP) aggregates various industrial loads to participate in DR, fully leveraging the flexible regulation capability of demand-side industrial users. First, we considered the load characteristics of multiple industrial users and establisheed regulation cost functions for three typical industrial users: electrolytic aluminum, steel, and cement. A cooperative game model was then constructed to coordinate the participation of industrial users in DR through VPP, with the Shapley value method employed to evaluate and allocate the profits of the cooperative alliance. Finally, simulation results show that by aggregating industrial users through VPP for DR participation, both the cooperative alliance and individual users experience a reduction in production costs, while the total response depth of the alliance also achieved an improvement.

Keywords: demand response; virtual power plant; cooperative games; industrial users; profit allocation

1. Introduction

The proposal and subsequent promotion of the “dual-carbon” objective has facilitated the large-scale integration of renewable energy sources, such as wind and photovoltaic power, into the energy grid. This development has established the foundation for a clean and low-carbon transformation of the energy system. By the end of June 2024, China’s installed wind and solar energy capacity had surpassed that of coal power [1]. However, the inherent stochastic and decentralized characteristics of

distributed renewable energy output have posed significant challenges to the balance between supply and demand in the power system, especially during the summer peak period and other times of high demand [2]. This has led to severe supply and demand conflicts, underscoring the urgent need to fully tap into the demand-side regulation potential to build a more flexible and reliable new power system.

Virtual power plants (VPPs) are emerging entities in power systems. They enhance flexibility and ease new energy integration by aggregating diverse resources [3]. These resources include distributed power, energy storage, and controllable loads. In demand response (DR), VPPs typically operate in two main ways: they can regulate the aggregated demand of consumers or dispatch resources owned by customers [4]. Industrial loads present a specific case. The regulation of their aggregated demand is a key opportunity for VPPs. Industrial facilities often possess significant schedulable loads. These loads, when centrally coordinated by a VPP, offer substantial flexibility for direct load control. In [5], a model-free DR dispatch strategy based on deep reinforcement learning was proposed for determining the optimal DR pricing strategy for VPPs. A multi-timescale scheduling model for VPPs considering capacity degradation of storage systems, carbon trading, and DR strategies was presented in [6]. The authors of [7] proposed a robust decomposition and tracking strategy for DR-enhanced VPPs to address the bias in DR. In [8], a multi-stage stochastic mixed-integer linear programming model was proposed to optimize the unit mix of power plants and virtual plants in the day-ahead and ancillary services markets. However, the DR aggregation of industrial users in power market transactions by VPPs has not been considered in the current study.

In recent years, DR technology has garnered considerable attention as a pivotal demand-side management tool [9]. By incentivizing users to adjust their electricity consumption during specific time periods, DR can effectively alleviate the differences in peak and off-peak loads, thereby improving the operational efficiency of power systems. Among these users, industrial consumers, with their high controllability and greater sensitivity to electricity costs, represent approximately 66% of the total electricity consumption [10]. While extensive adjustments to their entire operational load can be disruptive and costly, many industrial facilities possess specific processes or pieces of equipment that allow for short-term load reductions with minimal impact on overall production. Though this flexible portion may only constitute a part of their total demand, the sheer magnitude of industrial energy use means this adjustable capacity still represents a substantial resource for demand response. This characteristic, combined with their greater sensitivity to electricity costs, signifies considerable and often untapped potential for industrial DR participation. However, industrial demand response (IDR) is confronted by multifaceted challenges, including economic incentives, complex market and regulatory environments, and the inherent complexities and continuity requirements of industrial production processes [11]. A comprehensive overview of IDR status in Europe underscores its pivotal role in shaping future electricity systems and highlights the imperative for comprehensive solutions to address the challenges faced by industries in implementing DR programs [12]. Furthermore, a survey of industrial applications of demand response identifies high-potential industries like metals, cement, and refrigeration, and delineates the financial, regulatory, and knowledge-based impediments to widespread adoption [13].

Therefore, understanding how to effectively encourage industrial loads to participate in DR has become a topic of widespread interest. Pioneering work by Paulus & Borggrefe [14] assessed the technical and economic potential of demand-side management for energy-intensive industries in German electricity markets. Zarnikau et al. [15] analyzed how large industrial energy consumers in Texas respond to transmission costs based on the overlapping peak demand period during the summer months. To optimize energy management in industrial facilities, Ding et al. [16] proposed a demand response energy management scheme for smart grids, utilizing state-task networks and mixed-integer

linear programming to optimize scheduling and reduce energy costs. Schoepf et al. [17] explored how the availability of alternative production technologies affects the potential for industrial DR. In terms of the aggregator's role, Stede et al. [18] discussed how aggregators facilitate IDR in the German industrial sector. Rodríguez-García et al. [19] proposed a parallel particle swarm optimization algorithm to maximize the profit for industrial customers providing operation services in electric power systems. Oskouei et al. [20] presented an optimal scheduling method for demand response aggregators in industrial parks based on a load disaggregation algorithm. Zhao et al. [21] explored a multi-time scale DR scheme based on non-cooperative game theory for industrial parks equipped with integrated energy systems (IES). Tang et al. [22] studied demand bidding versus demand response for industrial electrical loads. Delving deeper into specific heavy industrial processes, Tu et al. [23] analyzed the energy consumption behavior and power characteristic modeling for the iron and steel industry, revealing the regularity of power fluctuations based on production process control. For isolated power systems, Liao et al. [24] proposed a coordinated control scheme for industrial energy-intensive loads, such as electrolytic aluminum, to utilize wind electricity locally and maintain frequency stability. Building upon this foundation, Wang et al. [25] further developed a grid interaction control strategy for electrolytic aluminum loads, considering process flow and regulation costs to ensure feasibility and minimize production impacts during grid interaction.

In summary, existing research has explored various aspects of industrial DR, including cost analysis, optimization algorithms, the role of aggregators, and bidding models, highlighting both the potential and the challenges associated with engaging industrial loads in DR programs. Existing studies have made significant progress in the scheduling strategies of VPPs, optimization methods for DR, and the potential of industrial users participating in DR. However, several issues remain unresolved:

(1) The adjustment costs associated with industrial users' participation in DR have not been effectively measured;
(2) Industrial users often participate in DR as independent entities, lacking effective aggregation;
(3) No effective solution has been proposed to aggregate multiple industrial users while simultaneously ensuring user benefits and adjustment depth.

In response to the limitations of the above-mentioned works, this paper considers the load characteristics of different types of industrial users, establishes the cost functions for regulating loads of each industrial user, and develops a cooperative game model coordinated by VPPs for users participating in DR. The model is solved using an improved L-PSO algorithm, and the Shapley value method is then applied to allocate profits among the industrial users participating in VPPs. The main contributions of this paper are as follows:

(1) For typical high-energy-consuming industrial users such as electrolytic aluminum, steel, and cement, this paper establishes cost functions that reflect the changes in the cost of each industrial user as their load regulation varies during DR participation, based on their respective production load regulation characteristics.
(2) To stimulate the DR potential of industrial loads and provide a profitable scheme for VPPs, a response mode is proposed in which VPPs lead the coordination of load regulation resources from multiple industrial users, reducing regulation costs and bundling their DR participation.
(3) A cooperative alliance among multiple industrial users is formed based on cooperative game theory. The group rationality and individual rationality of the cooperative game equilibrium ensure that both the cooperative alliance as a whole and each industrial user can achieve lower cost expenditures through cooperation.
(4) An improved PSO algorithm (L-PSO) is proposed, which incorporates a Levy flight mechanism for particles with poor fitness. This enhancement helps avoid local optima and accelerates the

convergence to the optimal load control scheme when solving the cooperative game model for VPP aggregation of multiple industrial users.

The remainder of this paper is organized as follows: Section 2 develops the cost function models for the varying response load depths of electrolytic aluminum, steel, and cement industrial users. Section 3 presents the cooperative game model and its constraints for aggregating multiple industrial users by VPPs in DR. Section 4 provides a simulation comparison and analysis of various scenarios for industrial user participation in DR. Section 5 provides a comprehensive conclusion to the paper.

2. Typical industrial users' adjustable load analysis

2.1. Electrolytic aluminum users

2.1.1. Electrolytic aluminum production load characteristics

Electrolytic aluminum production is a primary industrial method involving complex electrochemical processes. It is characterized by high and continuous electricity demand due to the large direct current, often several hundred kiloamperes, supplied to its electrolytic cells. These cells operate continuously at high temperatures, typically between 950 and 970 degrees Celsius, to maintain alumina in a molten state. A key operational characteristic relevant to demand response is their significant thermal inertia. This thermal inertia results from effective thermal insulation and allows the cells to tolerate temporary reductions in the supplied current without immediate critical temperature drops. Such tolerance offers a window for short-term load modulation. However, this flexibility is constrained because prolonged or excessive current reduction can lead to the solidification of the cryolite electrolyte, impacting the process. While short-duration current adjustments within tolerable limits generally incur minor costs, exceeding these operational boundaries or durations significantly impacts process stability and leads to escalating adjustment costs.

2.1.2. Electrolytic aluminum load adjustment cost

Electrolytic aluminum cells are powered by direct current (DC) converted from alternating current (AC) through transformers and rectifiers. Load regulation is achieved through several adjustments: modifying the high-voltage side voltage of the load bus, altering the transformation ratio of on-load tap-changing transformers, and controlling the voltage drop across saturable reactors. Reducing the current to 90% of its rated value results in a 10% capacity reduction; further capacity adjustment below this 90% level is not achievable. Moreover, operation below 75% of the rated current causes significant and detrimental sludging.

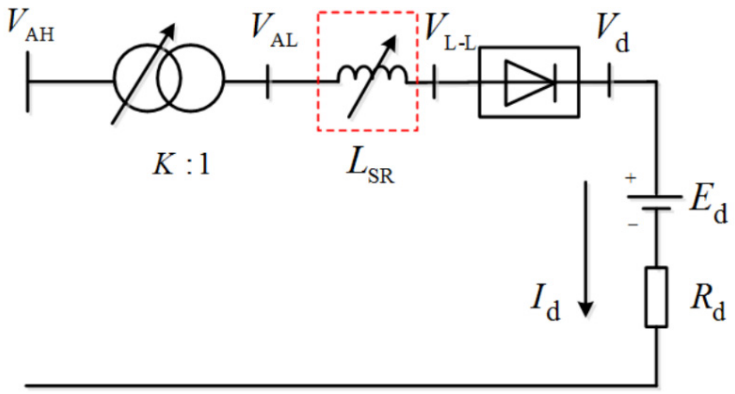

Figure 1. Equivalent circuit of electrolytic aluminum.

To participate in DR, electrolytic aluminum plants must adjust their cell operations. This paper models the cost of electrolytic aluminum load adjustment as a quadratic function of the adjusted power [26], as adopted in Eq (1):

$$C^a = \sum_{t=1}^{k} M_t^a \left(p_{a,t}^{typ} - p_{a,t}^{DR} \right)^2 \tag{1}$$

where C^a represents the total electrolytic aluminum adjustment cost over k DR periods. M_t^a is the cost coefficient at time t, which varies with the depth of current adjustment, as defined in Eq (2). I_t represents the ratio of the adjusted current at time t to the typical operating current. $p_{a,t}^{typ}$ and $p_{a,t}^{DR}$ denote the typical power consumption and the adjusted power consumption after DR participation at time t, respectively.

$$M_t^a = \begin{cases} M_{1,t}^a & 90\% < I_t \le 100\% \\ M_{2,t}^a & 75\% < I_t \le 90\% \\ M_{3,t}^a & I_t \le 75\% \\ M_{1,t}^a < M_{2,t}^a < M_{3,t}^a & \end{cases} \tag{2}$$

2.2. Steel users

2.2.1. Steel production load characteristics

In recent years, short-process steelmaking has rapidly developed, using recycled scrap steel as the primary raw material and electricity as the energy medium to melt scrap into steel through electric arc heating. Figure 2 illustrates the short-process steelmaking process, where the electric arc furnace (EAF) is the primary equipment involved in DR. EAFs function primarily as electric heating loads and, like most thermal loads, possess thermal inertia. Consequently, a brief emergency shutdown does not cause a sudden temperature drop. A buffer storage area is also typically present between the EAF and subsequent production stages. This buffer allows for short delays in restarting the EAF without

significantly impacting the overall production schedule. Therefore, steel users can participate in DR by adjusting EAF load.

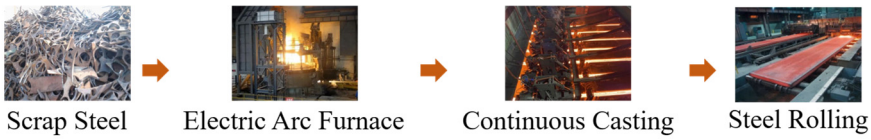

Figure 2. Schematic diagram of short-process steelmaking.

2.2.2. Steel load adjustment cost

Excessive EAF downtime leads to cooling of the furnace charge, resulting in additional electricity costs for reheating [27]. The adjustment cost of the EAF is related to the response duration. In this paper, it is assumed that when the response duration is short, the adjustment cost follows a linear function; conversely, when the response duration is long, the adjustment cost follows a quadratic function. As shown in Eq (3), this paper assumes that the adjustment cost, C^s, is a linear function when the EAF downtime is within t_s, with a cost coefficient of M_2^b. If the downtime exceeds t_s, the adjustment cost becomes a quadratic function with a cost coefficient of M_2^b. $p_{s,t}^{typ}$ represents the typical power consumption of the steel plant at time *t*, while $p_{s,t}^{DR}$ represents the adjusted power consumption after DR participation at time *t*.

$$C^s = \begin{cases} M_1^b \sum_{t=1}^{k} (p_{s,t}^{typ} - p_{s,t}^{DR}) & \triangle t < t_s \\ M_2^b \sum_{t=1}^{k} (p_{s,t}^{typ} - p_{s,t}^{DR})^2 & \triangle t \geq t_s \end{cases} \tag{3}$$

2.3. Cement users

2.3.1. Cement production load characteristics

Cement production involves four main steps, as illustrated in Figure 3: 1) Raw material preparation, including crushing and grinding; 2) Homogenization of raw materials into kiln feed; 3) Clinkerization, a high-temperature burning process in a kiln; and 4) Grinding of clinker and other materials. Electricity costs account for approximately 30% of the total production cost for cement users, providing considerable flexibility for load adjustment. The primary electrical loads in cement production include raw mills, cement mills, ball mills, rotary kilns, and vertical kilns, accounting for approximately 55% to 60% of the total load. These loads are primarily driven by electric motors, enabling rapid start-up and shutdown for DR participation.

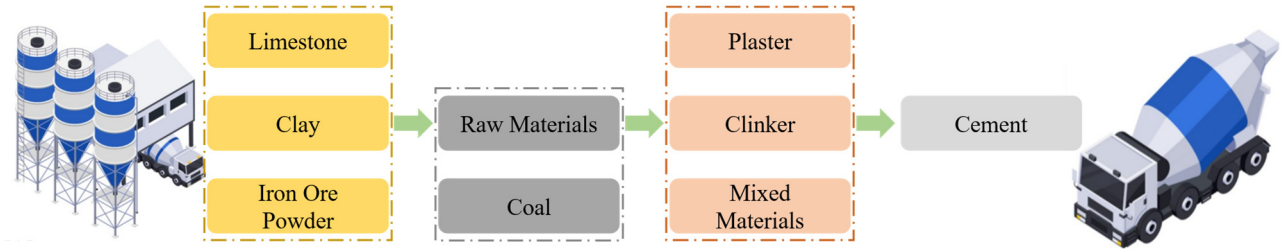

Figure 3. Schematic diagram of cement production.

2.3.2. Cement load adjustment cost

Due to the operational constraints on stopping or shifting electrical loads associated with the rotary kiln system under normal conditions, the DR capability of the rotary kiln is limited by other process arrangements and storage capacities. However, load adjustment of other mills has a relatively minor impact on the overall production process [28]. Figure 4 shows the load proportions of various cement production equipment. Therefore, we model the cement load adjustment cost as a piecewise linear function, as shown in Eq (4). If the adjustment amount, $\triangle p$, is less than or equal to the total load of mill-type equipment, p_c, the cost coefficient is M_1^c. If it exceeds, the cost coefficient becomes M_2^c. $p_{c,t}^{typ}$ represents the typical power consumption of the cement plant at time t, while $p_{c,t}^{DR}$ represents the adjusted power consumption after DR participation at time t.

$$C^c = \begin{cases} M_1^c \sum_{t=1}^{k} (p_{c,t}^{typ} - p_{c,t}^{DR}) & \triangle p \le p_c \\ M_2^c \sum_{t=1}^{k} (p_{c,t}^{typ} - p_{c,t}^{DR}) & \triangle p > p_c \end{cases} \tag{4}$$

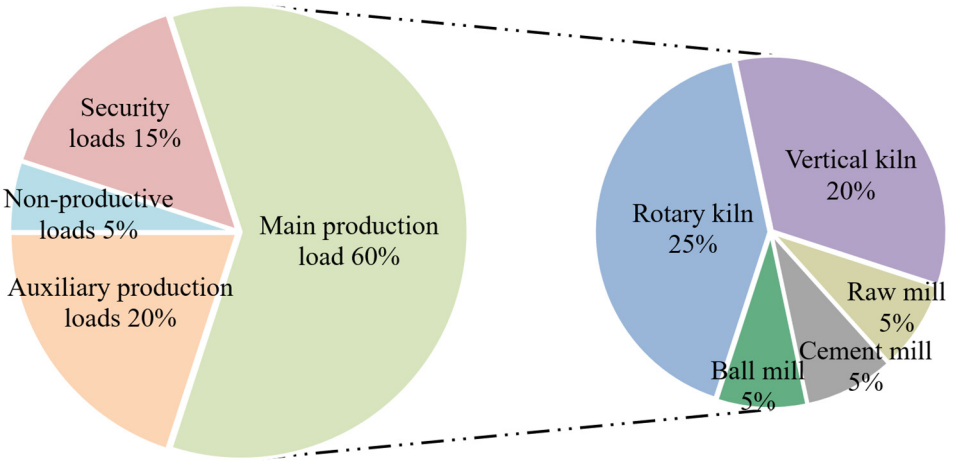

Figure 4. Cement load ratio.

3. Cooperative game model formulation and solution

3.1. Cooperative game model for multiple industrial users

3.1.1. Existence of a cooperative game

A cooperative game must satisfy group rationality and individual rationality [29]:

$$\forall S \subseteq N, \exists x \in X(S) : v(S) \geq \sum_{i \in S} v(\{i\}) \tag{5}$$

Group Rationality: For any subset S of the set of all players N, there exists a strategy profile x such that the payoff $v(S)$ achieved by all players in S cooperating is greater than or equal to the sum of their individual payoffs if they acted alone. Here, $v(\{i\})$ denotes the payoff player i obtains by acting independently.

$$\forall S \subseteq N, \forall i \in S, \exists x \in X(S) : v_i(x) \geq v(\{i\}) \tag{6}$$

Individual Rationality: For any subset of players S and any player i in S, there exists a strategy profile x such that player i's payoff $v_i(x)$ under this strategy profile is greater than or equal to the payoff $v(\{i\})$ they would obtain by acting independently.

Strategies satisfying both collective and individual rationality constitute the core solution of the cooperative game. For each industrial user, the decision variables are their electricity load profiles throughout the day, and the payoff function is defined as the reduction in their total daily production cost. Finding the core solution of the cooperative game amounts to finding strategies that allow the cooperating coalition to operate at a lower overall production cost.

3.1.2. Cooperation game model

In the cooperative game, the cooperative alliance involving DR by VPPs aggregating multi-industrial users is first considered as a whole. The overall maximum profit solution of the cooperative alliance is solved without considering the profit distribution of each participant within the alliance. The total profit of the cooperative alliance is shown in Eq (7):

$$min\, U_s = \sum_{k=1}^{n} C_e^k + C_a^k - B_{dr}^k \tag{7}$$

where U_s is the overall operating cost of the cooperative alliance for one day, n is the number of participating customers in the cooperative alliance, k represents the current customer number, C_e^k is the electricity cost of user k, C_a^k is the regulation cost of user k, and B_{dr}^k is the subsidy received by user k for participating in the DR.

The costs of electricity and DR subsidy components are shown in Eqs (8) and (9):

$$C_e^k = \sum_{t=1}^{m} p_t q_t^{k,DR} \tag{8}$$

$$B_{dr}^{k} = \sum_{t=1}^{o} (p_t^{typ} - p_t^{DR}) b \tag{9}$$

where m is the total number of time slots in a day, p_t is the tariff at time t, $q_t^{k,DR}$ is the load of user k after participating in DR at time t, o is the total number of time slots participating in DR, and b is the amount of subsidy per unit of load participating in DR.

3.2. Cooperative game response constraints

The aggregation of multiple industrial users through VPPs, in conjunction with their participation in DR within a cooperative game mode, necessitates the satisfaction of both the individual and cooperative operation constraints of each industrial user.

3.2.1. DR quantity balance constraint

The DR alliance has a total DR load equal to the sum of the adjustment amounts of each user during that period.

$$R_t^{VPP} = (r_t^a + r_t^s + r_t^c) \tag{10}$$

where R_t^{VPP} is the load response to be provided by the VPP at time t, and r_t^a, r_t^s, r_t^c are the respective response loads of electrolytic aluminum, steel, and cement users.

3.2.2. Total electricity consumption balance constraints

To ensure normal production, the total electricity consumption of each industrial user throughout the day should remain at the same level as before participating in the adjustment.

$$\begin{cases} \sum_{t=1}^{l} q_{a,t}^{typ} = \sum_{t=1}^{l} q_{a,t}^{DR} \\ \sum_{t=1}^{l} q_{s,t}^{typ} = \sum_{t=1}^{l} q_{s,t}^{DR} \\ \sum_{t=1}^{l} q_{c,t}^{typ} = \sum_{t=1}^{l} q_{c,t}^{DR} \end{cases} \tag{11}$$

where l is the total number of time periods in a day, $q_{a,t}^{typ}$, $q_{s,t}^{typ}$, $q_{c,t}^{typ}$ and $q_{a,t}^{DR}$, $q_{s,t}^{DR}$, $q_{c,t}^{DR}$ are the typical loads of electrolytic aluminum, steel, and cement users at time t and the electricity consumption after response adjustment, which ensures that the total electricity consumption of each industrial user is not affected after participating in DR.

3.2.3. Load regulation range constraints

The adjusted load of each industrial user should remain within the adjustable limit range.

$$\begin{cases} p_{min}^{a} \le p_{a,t}^{DR} \le p_{max}^{a} \\ p_{min}^{s} \le p_{s,t}^{DR} \le p_{max}^{s} \\ p_{min}^{c} \le p_{c,t}^{DR} \le p_{max}^{c} \end{cases} \tag{12}$$

where p_{min}^{a}, p_{min}^{s}, p_{min}^{c} are the minimum power of the load of electrolytic aluminum, steel, and cement users, respectively. p_{max}^{a}, p_{max}^{s}, p_{max}^{c} are the maximum power of the load of electrolytic aluminum, steel, and cement users, respectively.

3.2.4. Load response rate constraints

The load variation between adjacent periods should comply with the adjustment rate constraints of each industrial user.

$$\begin{cases} r_{down}^{a} \le p_{a,t}^{DR} - p_{a,t-1}^{DR} \le r_{up}^{a} \\ r_{down}^{s} \le p_{s,t}^{DR} - p_{s,t-1}^{DR} \le r_{up}^{s} \\ r_{down}^{c} \le p_{c,t}^{DR} - p_{c,t-1}^{DR} \le r_{up}^{c} \end{cases} \tag{13}$$

where r_{down}^{a}, r_{down}^{s}, r_{down}^{c} are the minimum response rates of electrolytic aluminum, steel, and cement users, respectively. r_{up}^{a}, r_{up}^{s}, r_{up}^{c} are the maximum response rates of electrolytic aluminum, steel, and cement users, respectively.

3.3. Benefit distribution based on the Shapley value approach

The Shapley value method is a solution for equitably distributing the benefits of a cooperative game based on the concept of marginal contribution. The method quantifies each participant's contribution to the collective effort by calculating the incremental benefits from their involvement across all possible coalition combinations. This calculation serves as the foundation for profit distribution, ensuring that each participant receives a return commensurate with their contribution and achieving a fair and reasonable distribution outcome. In summary, the Shapley value method calculates the "average contribution" of each participant in a cooperative endeavor. This method effectively addresses the issue of profit distribution in cooperative games and has found widespread application in economics, management, and related fields.

The Shapley value for user *i* is calculated by iterating over all possible coalitions *S* and quantifying the marginal contribution of user *i* when joining coalition *S*. Specifically, $v\left(S \cup \{i\}\right) - v\left(S\right)$ represents the incremental gain achieved by adding user *i* to coalition *S*. This difference is then weighted by the factor $\frac{|S|!\left(n-|S|-1\right)!}{n!}$ to account for the probability of user *i* joining coalition *S* at different positions within the permutation of all users. Finally, the Shapley value of user *i* is obtained by summing these weighted marginal contributions over all possible coalitions *S*. This procedure is formally defined in Eq (14):

$$\Phi_i = \sum_{S \subseteq N \setminus \{i\}} \frac{|S|!(n-|S|-1)!}{n!} \left[v(S \cup \{i\}) - v(S) \right] \tag{14}$$

where Φ_i denotes the Shapley value of user i, N represents the set of users participating in the game, $v(S)$ denotes the payoff of coalition S, n is the total number of users, and $|S|$ represents the cardinality (number of users) of coalition S.

3.4. PSO with Levy flight

Due to the presence of quadratic terms in the adjustment cost functions of industrial users in the cooperative game model, which exhibit strong nonlinearity, and the presence of numerous constraint terms, traditional mathematical programming methods face significant challenges in solving such complex, highly nonlinear problems. Additionally, when applying intelligent algorithms to solve these problems, there is a high risk of getting trapped in local optima. To address these challenges, this paper proposes an L-PSO algorithm for the cooperative game model with Levy flight perturbation updating for the last particles.

3.4.1. Levy flight

A Levy flight is defined as a random walk with a Levy distribution for the step size, and the probability distribution is heavy-tailed [30]. A distinguishing feature of Levy flights is the probability of a large stride during random walks, which differentiates them from Brownian motion. The inherent uncertainty in both movement distance and direction makes Levy flights a valuable component for swarm intelligence algorithms, especially for introducing random perturbations. These perturbations enhance the algorithm's global search capability. As illustrated in Figure 5, the trajectory of a Levy flight is characterized by its highly randomized direction and distance traveled. This randomization enables the perturbation to effectively explore all directions of the solution space, thereby escaping local optima during the algorithmic iteration process.

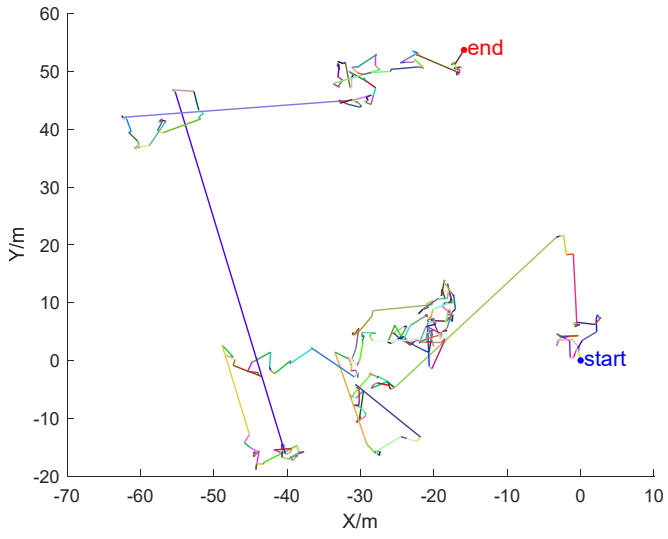

Figure 5. Example of Levy flight trajectory.

The generation of a random number that conforms to the Levy distribution is a challenging task. The Mantegna method is a common approach employed to extract the Levy flight step, as depicted in Eq (15). The step size s and the step size control factor α are multiplied together to update the particle position. The step size is calculated as shown in Eqs (16–18), where β is usually taken as 1.5.

$$x_i^{t+1} = x_i^t + \alpha \cdot s \tag{15}$$

$$\sigma_\mu = \left\{ \frac{\Gamma(1+\beta) \times sin(\frac{\pi\beta}{2})}{\Gamma(\frac{1+\beta}{2}) \times \beta \times 2^{\frac{\beta-1}{2}}} \right\}^{\frac{1}{\beta}} \tag{16}$$

$$\begin{aligned} &\sigma_v = 1 \\ &\mu \sim (0, \sigma_\mu{}^2) \\ &v \sim (0, \sigma_v) \end{aligned} \tag{17}$$

$$s = \frac{\mu}{|v|^{\frac{1}{\beta}}} \tag{18}$$

3.4.2. L-PSO algorithm searching process

In order to ensure the algorithm's convergence while enhancing its global search capability, L-PSO introduces Levy flights only for the few particles with the worst fitness in each iteration. These selected particles perform a Levy flight position update, while the rest of the examples continue to carry out the position updating of the standard particle swarm algorithm. The searching process of L-PSO is shown in Figure 6:

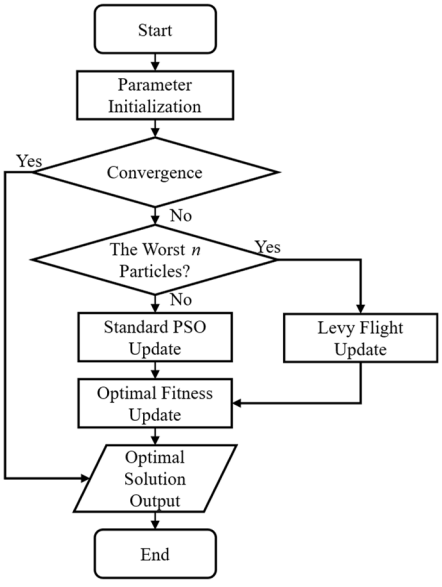

Figure 6. L-PSO solution process.

4. Comparative analysis of examples

In this section, different cases are set up to compare the response effects and economic benefits of industrial park users participating in DR individually or by joining a cooperative alliance in each case, and to explore the economic rationality of VPPs coordinating multiple industrial users to form a cooperative alliance.

4.1. Parameter settings

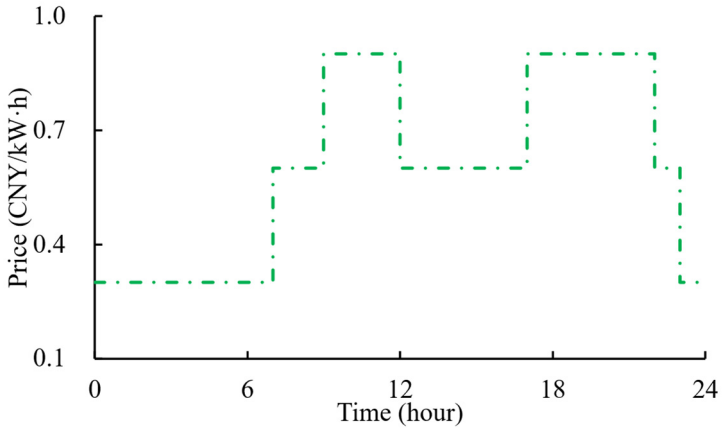

Figure 7. Electricity price.

This study assumes that each industrial user is subject to peak-valley electricity tariffs, with distinct peak and valley periods throughout the day as illustrated in Figure 7. The electricity tariffs are: Peak: 0.9 CNY/kW·h (09:00–12:00, 17:00–22:00); Valley: 0.4 CNY/kW·h (00:00–07:00, 23:00–24:00); Normal: 0.7 CNY/kW·h (remaining hours). Industrial users participate in DR through an invited peak-shaving program, committing to a designated response duration of 2 hours. The DR program is an incentive-based mechanism, offering a subsidy of 2500 CNY for every 1 MW-h of load response provided by participating users. For the case studies, User #1 represents an electrolytic aluminum plant, User #2 a steel mill, and User #3 a cement factory. Table 1 presents the different DR participation scenarios considered.

Table 1. Scenario settings for cases studies.

Cases	Response mode
Case 0	No DR participation
Case 1	Individual DR participation
Case 2	VPP aggregated Users #1, #2, and #3 participate in DR
Case 3	VPP aggregated Users #1 and #2 participate in DR
Case 4	VPP aggregated Users #1 and #3 participate in DR
Case 5	VPP aggregated Users #2 and #3 participate in DR

Cases 3–5 exemplifies a scenario in which a diverse group of users collaborates to engage in DR initiatives. The experiments are executed on a laptop computer that is equipped with a Windows 11 operating system, an Intel Core i9-13900HX CPU, and 16 GB RAM operating under the MATLAB R2024a software suite.

4.2. Performance validation of L-PSO

To rigorously evaluate the proposed L-PSO algorithm against a standard PSO alternative, a comparative performance analysis was conducted specifically within the context of the Case 2 scenario. This scenario, detailed in Table 1, involves the VPP aggregating electrolytic aluminum, steel, and cement users for cooperative participation in demand response, representing a key multi-user optimization problem from this study. For this direct comparison, both L-PSO and PSO algorithms were executed 10 independent times to solve the Case 2 optimization problem. Consistent parameters, including population size and a maximum of 100 iterations, were maintained for both algorithms to ensure a fair assessment of their capabilities on this specific application.

Table 2. PSO and L-PSO performance comparison for Case 2.

Performance indicator	PSO	L-PSO
Best fitness	1.450825×10^7	1.430843×10^7
Worst fitness	1.192503×10^{11}	1.470661×10^7
Mean final fitness	3.713859×10^{10}	1.449703×10^7
Std Dev final fitness	4.836949×10^{10}	1.425584×10^5

The statistical results from these 10 independent runs are summarized in Table 2 and highlight the practical advantages of L-PSO. L-PSO achieved a slightly better best fitness of 1.430843×10^7 compared to PSO's 1.450825×10^7. However, the most striking differences are observed in robustness and reliability. L-PSO's worst fitness, at 1.470661×10^7, is orders of magnitude superior to PSO's 1.192503×10^{11}, indicating a significantly reduced risk of converging to poor solutions. Furthermore, the mean final fitness for L-PSO is 1.449703×10^7, vastly better than PSO's 3.713859×10^{10}. Its standard deviation of final fitness, 1.425584×10^5, is also remarkably smaller than PSO's 4.836949×10^{10}. These metrics collectively demonstrate L-PSO's ability to consistently find high-quality solutions with much greater reliability.

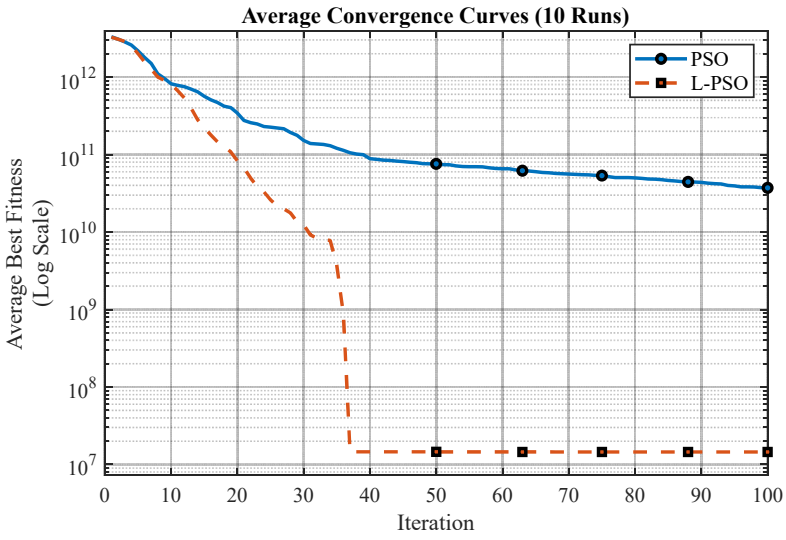

Figure 8. Convergence comparison of PSO and L-PSO for Case 2.

4.3. Comparison and analysis

The convergence characteristics, depicted in Figure 8, further substantiate L-PSO's superior performance. The figure plots the average best fitness over 100 iterations, with the *y*-axis on a logarithmic scale. It clearly shows that L-PSO, represented by the dashed orange line, converges significantly faster and to a substantially lower and better fitness value than PSO, shown by the solid blue line. L-PSO achieves a stable, near-optimal fitness by approximately the 40th iteration. In contrast, PSO exhibits much slower convergence and remains at a considerably higher fitness level even at the 100th iteration. A key reason for PSO's poorer performance and higher fitness values is its difficulty in effectively navigating the complex constrained solution space; it struggles to quickly eliminate substantial penalty terms associated with constraint violations, thereby hindering its rapid search for feasible and optimal solutions. This rapid convergence of L-PSO to a superior solution, coupled with its strong statistical performance, validates the effectiveness of the Levy flight mechanism in enhancing L-PSO's search capabilities for the complex VPP scheduling problem addressed.

In order to ascertain the cooperative approach with the optimal overall benefits, the overall benefits of cooperative alliances with different members are first compared. Taking the scenario in Case 1, in which each user participates in DR individually, as a benchmark, the corresponding user cost reductions are compared for several different cooperative scenarios in Cases 2–5. The results are presented in Table 3. It is evident that, in comparison with the individual response scenario depicted in Case 1, each cooperative scenario demonstrates the potential to achieve cost reductions. However, Case 2 involves a greater number of users participating in DR collectively, exhibits superior coordination in regulating load costs, effectively managing diverse load types, and attains enhanced economic benefits.

Table 3. Cost comparison for Cases 2–5.

Cases	Case 2	Case 3	Case 4	Case 5
Cost reduction (10^4 CNY)	2.75	1.85	0.03	0.99

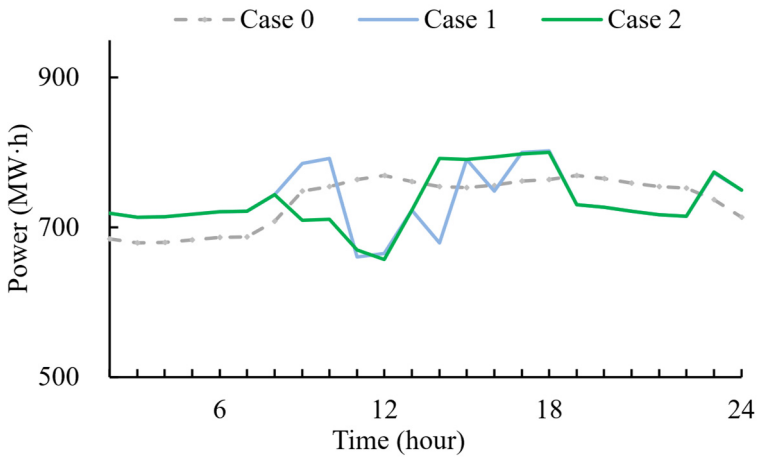

Figure 9. Electrolytic aluminum load under different cases.

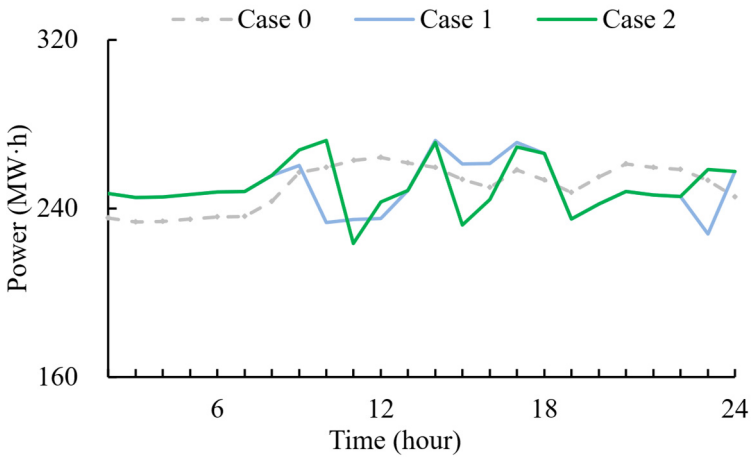

Figure 10. Steel load under different cases.

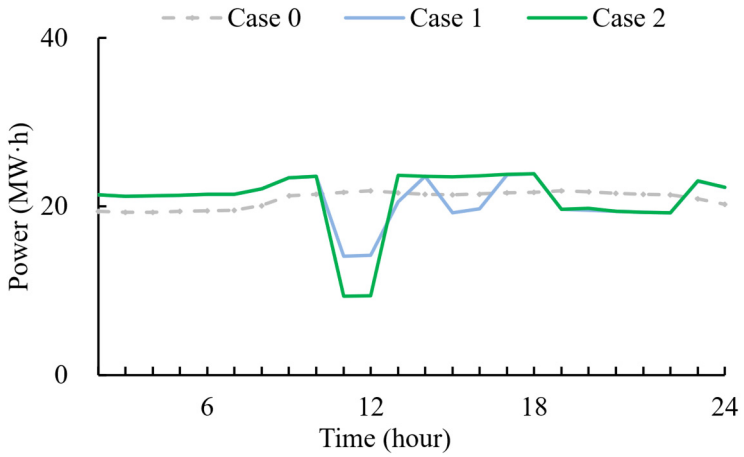

Figure 11. Cement load under different cases.

Figures 9–11 illustrate the all-day electricity load curves for each industrial user under different scenarios, facilitating a comparative analysis. Specifically, Case 0 in these figures represents the original load profile of each user without DR participation, serving as the baseline. Case 1 depicts load curves for individual DR participation, while Case 2 shows optimized load curves for VPP-aggregated participation. Comparing Case 1 and Case 2 against the Case 0 baseline clearly reveals the effects of DR.

It can be observed that compared to Case 1, in Case 2, the DR load of electrolytic aluminum users does not change significantly. The DR load of steel users increases by 6.2%, while that of cement users achieves a significant increase of 62.9%, and the total DR load of the cooperative coalition is improved by 11.5 WM·h.

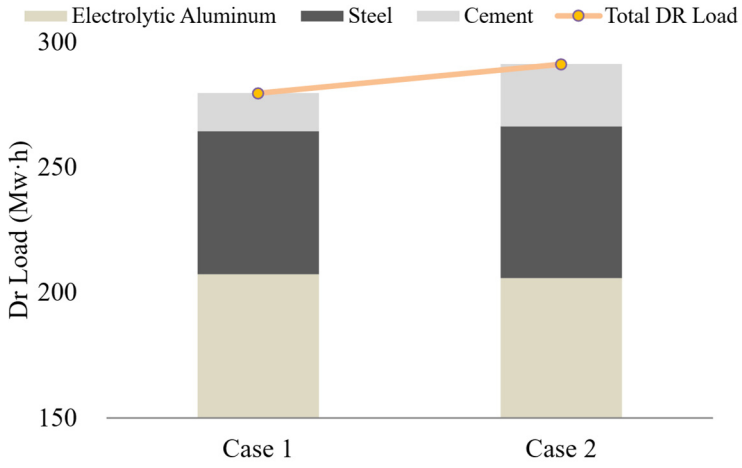

Figure 12. Comparison of DR load under 2 cases.

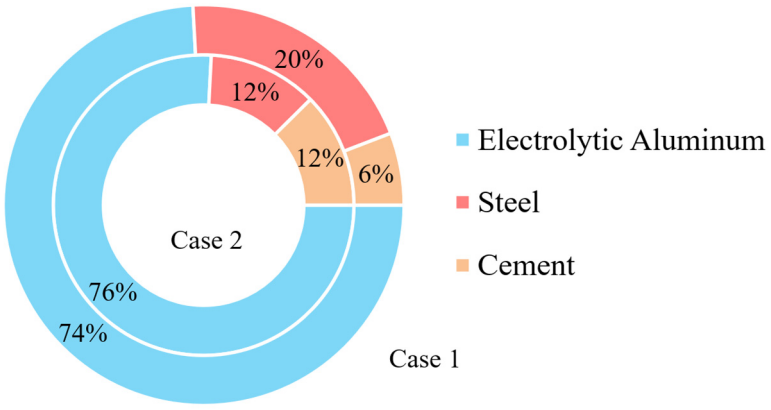

Figure 13. Comparison of adjustment costs under two cases.

Table 4. Cost comparison under different cases.

Cases	Aluminum cost (10^4 CNY)	Steel cost (10^4 CNY)	Cement cost (10^4 CNY)
Case 0	1053.35	358.53	29.06
Case 1	1030.48	350.78	27.60
Case 2	1030.04	349.75	26.33

As shown in Figures 12 and 13 and Table 4, the internal coordination within the cooperative alliance enhances the response depth of cement users. This prevents the situation where steel users, maintaining a high response volume for an extended period, would experience a sharp rise in regulation costs. For individual users, maintaining a certain response depth is required throughout their participation in DR. In the cooperative model, steel users can provide a brief deep response before

resuming production, with cement users supplementing the load. As a result, steel users' regulation costs are reduced by 43.0%, while cement users' regulation costs increase by 106.3%.

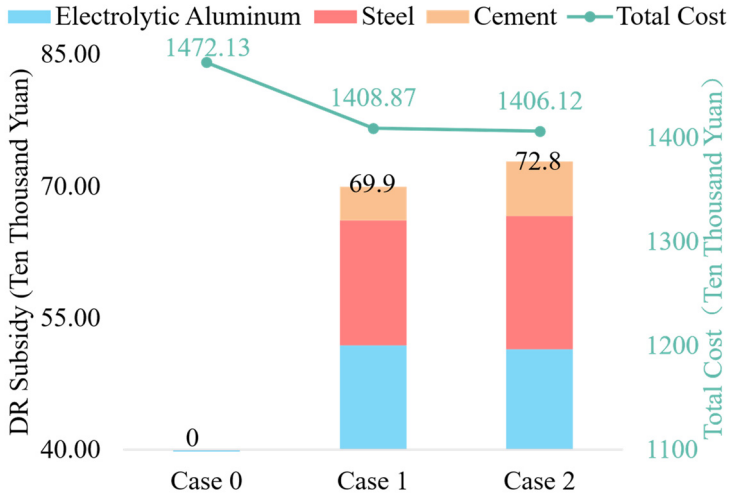

Figure 14. Comparison of DR subsidies and total costs in each case.

As shown in Figure 14, cement users' cost adjustments increase significantly after joining the cooperative alliance. However, costs are allocated based on each member's contribution. Due to their substantial load adjustments, cement users' contributions are high according to the Shapley value method, resulting in a larger share of the profits and reduced costs for both individual users and the entire alliance. Compared to Case 1, the cooperative alliance model in Case 2 offers notable advantages. It not only deepens the DR response but also leads to significant cost reductions. For instance, with 50 DR adjustments annually, the alliance's total operating costs can be reduced by 1.375 million RMB.

By aggregating multiple industrial users through VPPs to participate in DR, the cooperative alliance effectively coordinates load arrangements. This approach not only reduces costs for individual users and overall production costs within the alliance but also significantly enhances the depth of load response during DR participation. Furthermore, it creates reasonable profit margins for the VPP, facilitating its commercialization and operational sustainability.

5. Conclusions

This study examines the economic implications of multiple industrial users collaborating in DR aggregated by VPPs. Adjustment cost functions were developed for three typical industrial users—electrolytic aluminum, steel, and cement—based on their load characteristics. A cooperative game model was formulated and solved using an improved PSO with Levy flight, and profits were allocated using the Shapley value method. The model's effectiveness was verified through simulation cases, with key findings as follows:

(1) The simulation results show that the adjustment cost functions proposed in this study effectively refine the cost structure for industrial users, facilitating optimized load arrangements for each user.

(2) VPP aggregation of multiple industrial users significantly improves overall response capacity and optimizes load arrangements. Under the cooperative game framework, each user achieves greater

economic benefits compared to individual DR participation. Total costs are reduced, and the total response volume increases by 11.5 megawatt-hours. These outcomes highlight the dual benefits for both users and the power grid.

(3) The VPP aggregation strategy based on cooperative game theory not only enhances DR capacity but also generates a reasonable profit margin for both VPPs and users. With a fair distribution mechanism, VPPs can operate commercially without relying on additional subsidies.

Future research could expand the framework to include a wider range of industrial users and account for more complex market environments and uncertainties. Additionally, developing more refined cost adjustment functions and benefit allocation mechanisms tailored to diverse load characteristics could further improve the economic and social benefits for VPPs and industrial user alliances.

Use of AI tools declaration

The authors declare that no Artificial Intelligence (AI) tools have been used in the creation or revision of this article. The content is entirely the original work of the authors.

Acknowledgments

This work is supported by the Science and Technology Project of China Southern Power Grid Co., Ltd (ZBKJXM20240185).

Conflict of interest

The authors declare no conflicts of interest.

Author contributions

Long Wang: Conceptualization, Writing—original draft preparation, Project Administration; Tingzhe Pan: Methodology, Formal Analysis, Writing—review and editing, Supervision; Yi Wang: Investigation, Resources; Xin Jin: Data Curation; Heyang Yu: Software, Validation; Wangzhang Cao: Writing—review and editing. All authors have read and agreed to the published version of the manuscript.

References

1. Su W, Yi Y (2024) The maximum electricity load is expected to increase by 100 million kilowatts this year (in Chinese). *China Academic J Electron Publishing House*, 2024-07-26(002). Available from: https://link.cnki.net/doi/10.28061/n.cnki.ncdlb.2024.000949.
2. National Energy Administration (2023) China energy statistical yearbook 2023 (in Chinese). Beijing: China Statistics Press.
3. Chen H, Zhang H, Wang Z, et al. (2023) A review of market and scheduling characteristic parameter aggregation algorithm of different types of virtual power plants (in Chinese). *Proc CSEE*, 43: 15–28. Available from: https://link.cnki.net/doi/10.13334/j.0258-8013.pcsee.212744.
4. Wu X, Yang M, Liang L, et al. (2025) Redesign of virtual power plant-led electricity demand response program. *Prod Oper Manage* 34: 1817–1835. https://doi.org/10.1177/10591478241305859

5. Kuang Y, Wang X, Zhao H, et al. (2023) Model-free demand response scheduling strategy for virtual power plants considering risk attitude of consumers. *CSEE J Power Energy Syst* 9: 516–528. https://doi.org/10.17775/CSEEJPES.2020.03120
6. Li Q, Zhou YC, Wei FC, et al. (2024) Multi-time scale scheduling for virtual power plants: Integrating the flexibility of power generation and multi-user loads while considering the capacity degradation of energy storage systems. *Appl Energy* 362: 122980. https://doi.org/10.1016/j.apenergy.2024.122980
7. Pang S, Xu Q, Yang Y, et al. (2024) Robust decomposition and tracking strategy for demand response enhanced virtual power plants. *Appl Energy* 373: 123944. https://doi.org/10.1016/j.apenergy.2024.123944
8. Fusco A, Gioffre D, Castelli AF, et al. (2023) A multi-stage stochastic programming model for the unit commitment of conventional and virtual power plants bidding in the day-ahead and ancillary services markets. *Appl Energy* 336: 120739. https://doi.org/10.1016/j.apenergy.2023.120739
9. Fan S, Wei Y, He G, et al. (2022) Discussion on demand response mechanism for new power systems (in Chinese). *Auto Electr Power Syst* 46: 1–12. Available from: https://link.cnki.net/urlid/32.1180.TP.20220126.1425.008.
10. Annual Development Report on China's Electric Power Industry 2023 (Abstract) (2023) (in Chinese). *China Electic Power News*. Available from: https://link.cnki.net/doi/10.28061/n.cnki.ncdlb.2023.000819.
11. Dai X, Chen H, Xiao D, et al. (2022) Review of applications and researches of industrial demand response technology under electricity market environment (in Chinese). *Power Syst Technol* 46: 4169–4186. Available from: https://link.cnki.net/doi/10.13335/j.1000-3673.pst.2022.1328.
12. Ranaboldo M, Aragüés-Peñalba M, Arica E, et al. (2024) A comprehensive overview of industrial demand response status in Europe. *Renewable Sustainable Energy Rev 2*03: 114797. https://doi.org/10.1016/j.rser.2024.114797
13. Shoreh MH, Siano P, Shafie-khah M, et al. (2016) A survey of industrial applications of demand response. *Electr Power Syst Res* 141: 31–49. https://doi.org/10.1016/j.epsr.2016.07.008
14. Paulus M, Borggrefe F (2011) The potential of demand-side management in energy-intensive industries for electricity markets in Germany. *Appl Energy* 88: 432–441. https://doi.org/10.1016/j.apenergy.2010.03.017
15. Zarnikau J, Thal D (2013) The response of large industrial energy consumers to four coincident peak (4CP) transmission charges in the Texas (ERCOT) market. *Util Policy* 26: 1–6. https://doi.org/10.1016/j.jup.2013.04.004
16. Ding YM, Hong SH, Li XH (2014) A demand response energy management scheme for industrial facilities in smart grid. *IEEE Trans Ind Inf* 10: 2257–2269. https://doi.org/10.1109/TII.2014.2330995
17. Schoepf M, Weibelzahl M, Nowka L, et al. (2018) The impact of substituting production technologies on the economic demand response potential in industrial processes. *Energies* 11: 2217. https://doi.org/10.3390/en11092217
18. Stede J, Arnold K, Dufter C, et al. (2020) The role of aggregators in facilitating industrial demand response: Evidence from Germany. *Energy Policy* 147: 111893. https://doi.org/10.1016/j.enpol.2020.111893
19. Rodríguez-García J, Ribó-Pérez D, Alvarez-Bel C, et al. (2020) Maximizing the profit for industrial customers of providing operation services in electric power systems via a parallel particle swarm optimization algorithm. *IEEE Access* 8: 24721–24733. https://doi.org/10.1109/ACCESS.2020.2970478

20. Oskouei MZ, Zeinal-Kheiri S, Mohammadi-Ivatloo B, et al. (2022) Optimal scheduling of demand response aggregators in industrial parks based on load disaggregation algorithm. *IEEE Syst J* 16: 945–953. https://doi.org/10.1109/JSYST.2021.3074308
21. Zhao W, Ma K, Guo J, et al. (2024) A multi-time scale demand response scheme based on noncooperative game for economic operation of industrial park. *Energy* 302: 131875. https://doi.org/10.1016/j.energy.2024.131875
22. Tang X, O'Neill R, Hale E, et al. (2024) Demand bidding vs. demand response for industrial electrical loads. *Comput Chem Eng* 189: 108768. https://doi.org/10.1016/j.compchemeng.2024.108768
23. Tu X, Xu J, Liao S, et al. (2018) Process controlling based energy consumption behavior analysis and power characteristic modeling for iron and steel industry (in Chinese). *Auto Electr Power Syst* 42: 114–120. Available from: https://link.cnki.net/urlid/32.1180.TP.20171123.0934.010.
24. Liao S, Xu J, Sun Y, et al. (2018) Local utilization of wind electricity in isolated power systems by employing coordinated control scheme of industrial energy-intensive load. *Appl Energy* 217: 14–24. https://doi.org/10.1016/j.apenergy.2018.02.103
25. Wang X, Chen B, Xie H, et al. (2025) Participation of electrolytic aluminum loads in grid interaction control strategies considering process flow and regulation costs. *Front Energy Res* 12: 1493558. https://doi.org/10.3389/fenrg.2024.1493558
26. Du S, Huang Y, Liu R, et al. (2023) Integrated energy management approach for photovoltaic power station-thermal unit-aluminum electrolysis plant islanded microgrids for multi-time scale (in Chinese). *Hunan Electr Power* 43: 37–44. https://doi.org/10.3969/j.issn.1008-0198.2023.06.007
27. Ranaboldo M, Aragüés-Peñalba M, Arica E, et al. (2024) A comprehensive overview of industrial demand response status in Europe. *Renewable Sustainable Energy Rev* 182: 106358. https://doi.org/10.1016/j.rser.2024.114797
28. Golmohamadi H (2022) Demand-side management in industrial sector: A review of heavy industries. *Renewable Sustainable Energy Rev* 158: 112046. https://doi.org/10.1016/j.rser.2021.111963
29. Dekel E, Gul F (1997) Rationality and knowledge in game theory. *Econometr Soc Monogr* 26: 87–172.
30. Li J, An Q, Lei H, et al. (2022) Survey of Lévy flight-based metaheuristics for optimization. *Mathematics* 10: 2785. https://doi.org/10.3390/math10152785

AIMS Press